

# Structural investigations of SiO–CeO<sub>2</sub> thin films

A. SINGH, C. A. HOGARTH

*Department of Physics, Brunel University, Uxbridge, Middlesex, UK*

Aspects of the structure of vacuum co-evaporated SiO–CeO<sub>2</sub> thin films are elucidated by first presenting the optical transmission edges for a series of such films. These show a differentiation into two distinct groups, and the presence of weak absorption minima, possibly defect-induced, confined to one of these groups. Previously obtained infrared (IR) results are compared with these UV results, and the IR evidence for the O<sub>1</sub><sup>0</sup> and O<sub>3</sub><sup>+</sup> defect centres associated with oxygen sites is noted. The electron spin resonance (ESR) results for pure a-SiO thin films are then discussed in terms of those of vitreous SiO<sub>2</sub>, and it is concluded that only O<sub>1</sub><sup>0</sup> and O<sub>3</sub><sup>+</sup> ESR-related defect centres exist in amorphous SiO films in significant quantities. It is also concluded that adding CeO<sub>2</sub> to the films reduces the O<sub>1</sub><sup>0</sup> concentrations via chemical bonding, while the O<sub>3</sub><sup>+</sup> centres remain unaffected. Finally it is shown that the separate identity of any possible defect-induced optical absorption bands in the series from those expected for a-SiO and CeO<sub>2</sub> can be used as new evidence for the presence of Si–Ce bonding.

## 1. Introduction

In an earlier paper [1] we reported the infrared (IR) spectroscopic investigation of a series of vacuum-evaporated SiO–CeO<sub>2</sub> thin films prepared by the co-evaporation of the two oxides on to the same substrate. Interest in such films has arisen from their possible use as dielectrics in metal–insulator–metal (MIM) structures [2]. Electron spin resonance (ESR) measurements on the same series of films have also been made [3] and in addition Hogarth and Al-Dhhan [4] have briefly studied the nature of their optical band-gap  $E_{\text{opt}}$ .

The aim of the IR investigation was to elucidate the chemical nature of the films. It was subsequently decided to broaden this study to the analysis of their structure. To this end the optical measurements were extended to include a more comprehensive range of samples, and attention was directed to the general form of the optical spectra rather than to the calculation of  $E_{\text{opt}}$ . In this paper the results of these measurements are first presented and discussed. The results of all three types of measurement are then compared with each other and with those of similar work by others in an attempt to gain a clearer picture of the structural nature of the films. Special attention is directed towards the identification of the defect centres in a-SiO thin films, and how these are modified with the addition of CeO<sub>2</sub>.

## 2. Experimental procedure

The thin-film samples for the optical measurements were prepared concurrently with the IR samples described earlier [1]. Corning 7059 glass pieces 2.5 cm × 2.5 cm in area were used as substrates. The preparation conditions of substrate temperature, ambient vacuum and deposition rates were the same as for the corresponding IR samples.

The UV spectra were run on a Perkin-Elmer

Lambda 9 UV/VIS/NIR spectrophotometer over the 185 to 800 nm range for the unannealed samples and 200 to 800 nm for the annealed samples.

Annealing of the optical samples was performed for two hours at 200°C at a pressure of  $1 \times 10^{-5}$  torr in the same vacuum chamber as that used for their preparation. Once again this was carried out concurrently with the annealing of the IR samples.

## 3. Results and discussion

### 3.1. Optical transmission spectra

Fig. 1 shows the normalized optical transmission edges of the eleven different SiO–CeO<sub>2</sub> thin films considered in this work. The edges have been normalized to a thickness of 300 nm by first calculating the absorption constant  $\alpha$  using the relation

$$I_t = I_0 e^{-\alpha t}$$

where  $t$  is the thickness, and then re-calculating the transmittance  $I_t/I_0$  at the new thickness of 300 nm using the same relation. It is seen that the edges divide themselves into two groups, the first manifesting those edges belonging to films with SiO content ranging between 78 mol % SiO–22 mol % CeO<sub>2</sub> and 51 mol % SiO–49 mol % CeO<sub>2</sub> inclusive, and the second group displaying the remaining edges. The former group is characterized by greater transparency at higher photon energies, as well as the presence of transmission minima. Fig. 2, containing the un-normalized edges, reveals these minima more clearly. In contrast to the first group, the latter group of edges “become absorbing” at lower photon energies (higher wavelengths) have smooth featureless slopes and exhibit almost total absorption at the highest photon energies.

The presence of interference effects (not shown in the figures) at longer wavelengths in these optical spectra allows the estimation of their refractive indices

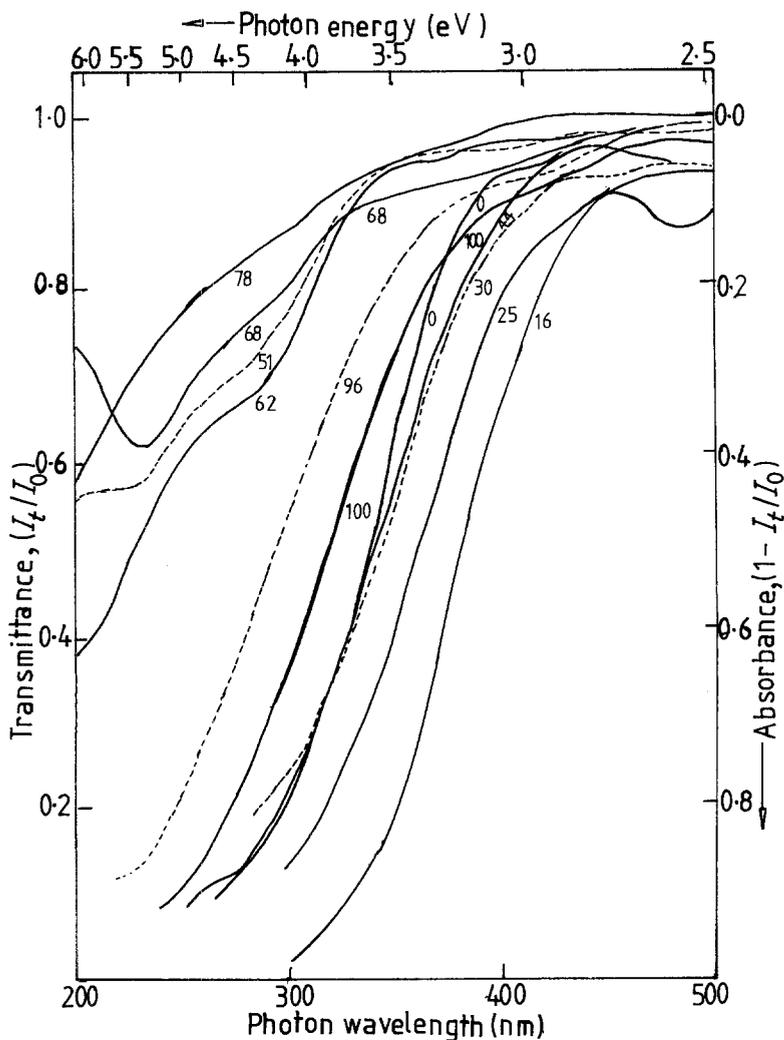


Figure 1 Optical transmission edges of SiO-CeO<sub>2</sub> thin films normalized to an effective film thickness of 300 nm. The numbers indicate film compositions in (mol % SiO).

$n$  and dielectric constants  $\epsilon$  using the relations

$$(2nd)^{-1} = \lambda_{m+1}^{-1} - \lambda_m^{-1}$$

and

$$\epsilon = n^2$$

where  $d$  is the film thickness,  $\lambda$  is the photon wavelength and  $m$  is the order of the interference fringe [5, 6]. Table I lists the average values for such constants over the wavelength ranges indicated. Comparison of the last entry in this Table to Table 2 of Al-Ani and Beynon [5] shows that the 100 mol % SiO film may have sustained a small degree of oxidation during the preparation process, though this is of little consequence to the present aims.

Apart from the features already noted, the first group of edges also shows the formation of a distinct new "shoulder" at ca. 340 nm. As pointed out by Connell [7] the electronic energy band widths in both crystalline and amorphous solids are decided largely by the order within the "molecular units" forming the solid. In fact Kastner [8], following the observations of Mooser and Pearson [9], Cohen and Heine [10], Meyer [11] and Friederich [12, 13] on the merits of using the chemical bonding picture in enumerating the band structure of solids, has suggested that these bands may be considered to be broadened superpositions of the bonding, antibonding and lone-pair energy levels of such molecular units. This fact has been very successfully utilized by many subsequent workers in

visualizing the bandgap properties of solids. Early experimental demonstrations of the role of "molecular units" in deciding the optical properties of both crystalline and amorphous states are provided by the works of Joffé and Regel [14] and Philipp [15]. The new shoulder in the transmission edges seems to indicate the formation of an optical energy gap  $E_{opt}$  different from that of pure a-SiO or a-CeO<sub>2</sub>. Thus this may be a manifestation of a new chemical bond between the elemental components of the films (with its respective bonding and antibonding orbitals giving rise to new conduction and/or valence bands).

The occurrence of the transmission minima at discrete frequencies, rather than being randomly distributed over the frequency range, seems to indicate that they are not macroscopic optical effects caused by such things as large voids. Instead they appear to be absorption bands caused by intrinsic structural defects in the solid. However, residual absorption by the substrate and the presence of impurities cannot be ruled out as other possible causes. Thus the band at

TABLE I Estimates of refractive indices  $n$  and dielectric constants  $\epsilon$  for films of representative compositions

Film composition (mol % SiO)	Wavelengths at maxima (nm)	Average $n$ over intervals	Dielectric constant, $\epsilon$
0	444, 508, 600	2.41, 2.27	5.83, 5.15
25	456, 540	1.58	2.48
100	480, 635	1.67	2.77

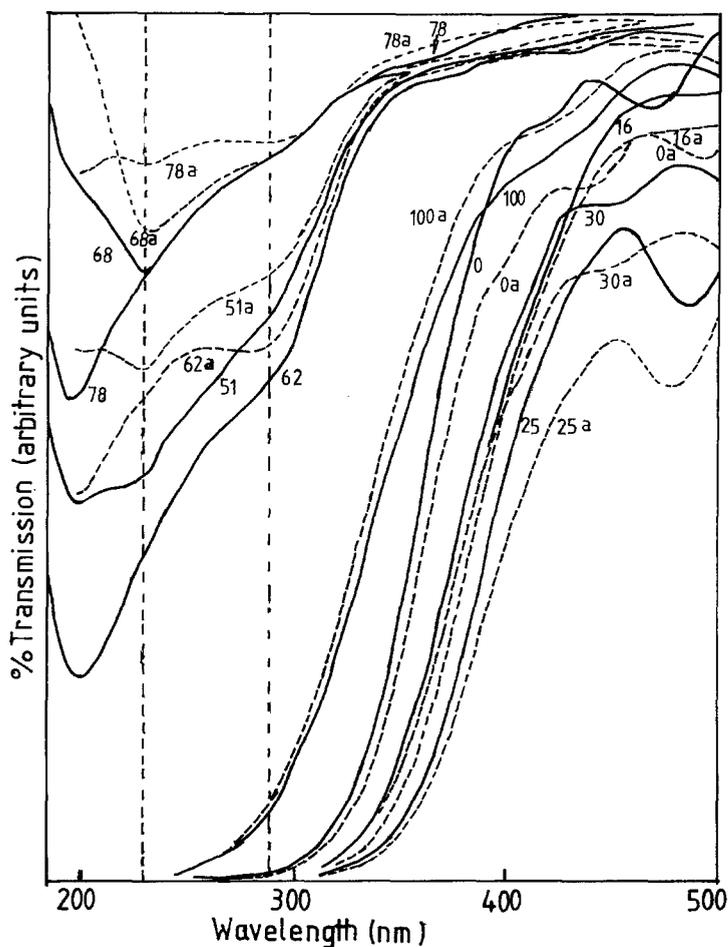


Figure 2 Optical edges of SiO-CeO<sub>2</sub> thin films (—) before and (---) after annealing. The letter "a" following the value of a film composition indicates annealing.

200 nm appears almost certainly to be substrate-related, and must be ignored. The band at 290 nm, on the other hand, cannot be similarly caused and deserves serious attention. These minima will be discussed further after the ESR results have been interpreted.

The second group of edges are best discussed in relation to the pure CeO<sub>2</sub> edge. The progressive advancement of the edges along the wavelength axis is probably a direct reflection of the change in film composition, with ensuing changes in absorbance, with the addition of SiO. However the sudden change between the pure CeO<sub>2</sub> edge and the 16 mol % SiO edge can only be explained in terms of disorder changes. The former film is expected to be much more ordered than that prepared by Al-Dhhan [16] because the deposition rate here of 0.5 nm sec<sup>-1</sup> was much slower than the 1.7 nm sec<sup>-1</sup> of his earlier work. Also, in contrast to the result of Al-Dhhan, the present edge does not follow the absorption rule

$$\alpha(\omega) = \frac{B}{\hbar\omega} (\hbar\omega - E_{\text{opt}})^2$$

proposed by Tauc *et al.* [17] and Davis and Mott [18] for many non-crystalline materials. Thus the sudden shift in the edge to longer wavelength with SiO addition is probably due to an increase in disorder caused by the presence of the small amount of SiO.

Annealing of the films was carried out in an attempt to reduce the density of the gap states so that the band edges might become clearer. Though some of the anticipated effect did take place (e.g. at the "shoulder"

regions) it was not nearly as pronounced as expected. This provides a first indication that the types of disorder responsible for the gap states are more complex than the simple dangling bonds conceived originally.

The effect of annealing on films lower in SiO concentration than 51 mol % SiO contrasts markedly with SiO-rich films. Instead of sharpening the shoulders, annealing has the opposite effect here. In fact the new edges formed after annealing are characteristic of more disordered structures, indicating that the heat treatment increased rather than decreasing the structural disorder. A possible explanation is that the films of this group were initially much more ordered than the others, and that annealing was effective in destroying some of this order through a process of thermal randomization. In any event it is seen that annealing provides a further method of dividing the films into two distinct groups, each with its own properties.

### 3.2. Comparison of IR and UV spectra

The fact that the division of the transmission edges into two groups at a composition of 51 mol % SiO is almost coincident with the disappearance of the 876 cm<sup>-1</sup> IR band after the 44 mol % SiO value is a clear indication that the characteristics of the first group of films are somehow associated with large concentrations of non-bridging oxygen (NBO) atoms. In all probability these SiO-rich films contain an excess of SiO over the concentrations required for bonding with CeO<sub>2</sub>. This state of affairs would lead to the presence of the detected NBO atoms.

Comparisons of IR and UV results are also useful

in elucidating the nature of the defect centres in the films. Any defect-induced minima in the transmission spectra of the first group of films may be due to any of several different possible types of defect. Their correlation with specific defects is difficult (but is discussed later). The IR band at  $876\text{ cm}^{-1}$ , however, does single out one class of defects contributing to the optical spectra. Since the IR band is due to the vibrations of singly co-ordinated oxygen atoms, some gap states must therefore be due to electronic configurations (elaborated later) associated with such atoms. Thus the IR results act as an independent proof of the existence of such defects, an example of vibrational measurements helping to elucidate electronic properties. It will be seen below that weak bands in the  $600\text{ to }700\text{ cm}^{-1}$  region may provide evidence for yet another type of electronic defect in a-SiO.

### 3.3. ESR and defect centres in a-SiO

Disorder in amorphous solids may be classified into topological disorder [19, 20] comprising changes in orientations and bond lengths of the molecular units, and defects due to broken bonds and the formation of "wrong" bonds. The first category gives rise to the general features of the density of states, the most important being band tailing [19, 20]. In the case of vitreous  $\text{SiO}_2$  (v-SiO<sub>2</sub>) the other category, namely the defect centres, has been described by O'Reilly and Robertson [21] in terms of two models, the valence alternation (VA) model and the vacancy bridge (VB) model. The VB model for v-SiO<sub>2</sub> views defects as arising from Frenkel-type defects of the oxygen atom, leading to the neutral oxygen vacancy  $\text{Si}^{\cdot}\text{Si}$  and the peroxy bridge  $\text{Si}-\text{O}-\text{O}-\text{Si}$ , which forms the precursor to the important peroxy radical  $\text{Si}-\text{O}-\text{O}^{\cdot}$  [22]. The VA model, on the other hand, views defects as arising from broken Si-O bonds, and the possible subsequent transformations of these into other charged or neutral centres [23-30]. Fig. 3 shows the VA defects of relevance here, together with their symbols. As indicated there symbolically,  $\text{Si}_4^0$  and  $\text{O}_2^0$  refer to normal, fully coordinated silicon and oxygen atoms (i.e. a silicon atom bonded to four oxygen atoms, respectively);  $\text{Si}_3^0$  and  $\text{O}_1^0$  are neutral under-coordinated atoms each possessing a dangling bond, and  $\text{Si}_3^+$ ,  $\text{O}_1^-$  are under-coordinated charged sites. The  $\text{O}_3^+$  centre is formed when an  $\text{Si}_3^0$  or  $\text{Si}_3^+$  centre reacts with a neighbouring  $\text{O}_2^0$  centre with or without the liberation of an electron. Because of the chemical similarity between a-SiO thin films and v-SiO<sub>2</sub>, one would expect at least some of the defects in v-SiO<sub>2</sub> to be present in a-SiO as well.

Since many of these defects possess unpaired electrons, they form paramagnetic centres and can thus be identified using ESR. In the present context such measurements on a-SiO show the existence of only one paramagnetic centre. The evidence considered so far suggests that it could be  $\text{O}_1^0$  or  $\text{Si}_3^0$  or both. To elucidate the exact nature of the defects in a-SiO, one must reconsider v-SiO<sub>2</sub> and inspect the ESR studies of this material by Lucovsky [27, 28, 30]. Following the

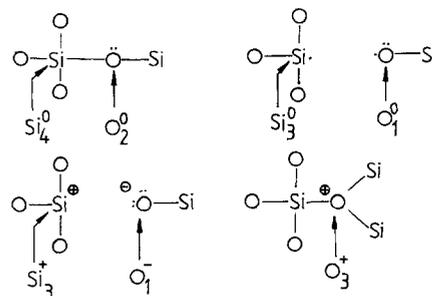
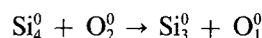


Figure 3 Possible defect centres in  $\text{SiO}_2$  arising from broken Si-O bonds. The first diagram shows normal silicon and oxygen sites in the  $\text{SiO}_2$  CRN.

pioneering efforts of Anderson [31], Street and Mott [32], Kastner, *et al.* [33] and Kastner and Fritzsche [34] on the nature of the non-paramagnetic centres in chalcogens, and of Griscom [35] and Greaves [36, 37] on the electronic defects and colour centres in v-SiO<sub>2</sub>, Lucovsky has carried out a thorough investigation of the VA type of defect in v-SiO<sub>2</sub>. Here no paramagnetic centres are found in pristine v-SiO<sub>2</sub>, but two different centres, namely the  $E'$  centre (which is identical with  $\text{Si}_3^0$ ) and the oxygen hole centre OHC (which has been identified as  $\text{O}_1^0$ ) arise after the specimen is gamma-irradiated. Starting with the creation of  $\text{Si}_3^0$  and  $\text{O}_1^0$ , Lucovsky [27] explains the non-existence of paramagnetic centres in pristine v-SiO<sub>2</sub> by first showing that the formation of this pair by itself is energetically unfavoured, since the reaction



requires an energy expenditure of  $E = E_b + E'_b$ , where  $E_b \approx E'_b \approx 5\text{ eV}$ , of the order of half the bond dissociation energy of the Si-O bond. The energetics of such defect formation/transformation are best understood in terms of the energy level diagrams for the respective bonding configurations given by Lucovsky [28] and reproduced here in Fig. 4. In these

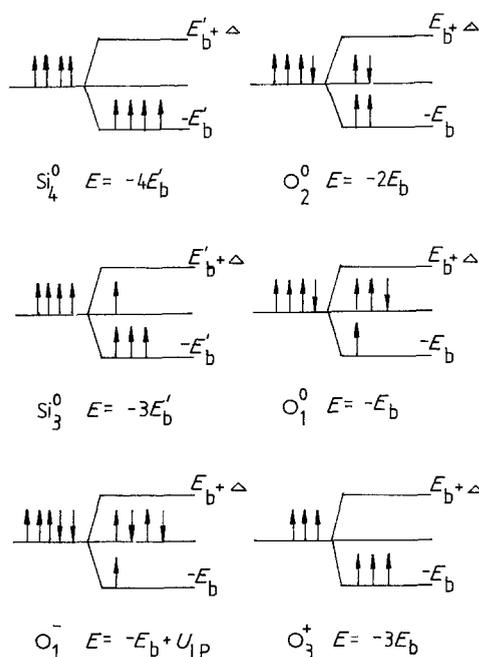
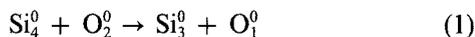


Figure 4 Bonding configuration energies of silicon and oxygen defect centres in  $\text{SiO}_2$  (after Lucovsky [28]). See text for explanation. ( $\Delta$  is a small energy difference.)

diagrams the horizontal lines on the left represent valence atomic orbital energy levels and those on the right the corresponding molecular bonding, lone-pair and antibonding orbital energies. The arrows depict electron occupancies, and  $E$  denotes the total energy required to form the molecular bonds from the respective atomic orbitals.

Lucovsky next demonstrates that it is energetically more feasible for such a pair to give rise to a charged defect pair through the following steps:



i.e.  $2\text{O}_2^0 \rightarrow \text{O}_3^+ + \text{O}_1^-$ . In Step 2 a triply coordinated neutral silicon atom combines with a neighbouring doubly coordinated oxygen atom, liberating an electron in the process and producing a triply coordinated oxygen centre. In Step 3 the liberated electron is captured by the  $\text{O}_1^0$  centre nearby, producing two neighbouring charged centres, dubbed an "intimate valence alternation pair" or IVAP by Lucovsky. The whole process requires an energy expenditure of  $U_{\text{LP}}$  (the electron-pair repulsion energy between oxygen lone-pair electrons,  $\approx 2\text{ eV}$ ) only. In a later paper, Lucovsky [28] shows how, after gamma irradiation, these centres are able to trap photogenerated holes and electrons and reproduce the stable  $E'$  and OHC centres.

Besides the ESR centres mentioned above, Friebele *et al.* [38] and Griscom and Friebele [39] have also discovered the presence of the peroxy radical in neutron-irradiated and annealed  $v\text{-SiO}_2$ .

Returning to the  $a\text{-SiO}$  thin films, the chemical bonding found here is on the whole expected to be similar to that of  $v\text{-SiO}_2$ , although a greater proportion of Si-Si bonds is anticipated. Because of the history of formation of these films, however, the overall structure should be significantly different from that of the bulk [40]. One expects a good proportion of dangling bonds on silicon and oxygen atoms to be preserved *in situ* after condensation from the gaseous state, steric hindrance being significant in SiO. This contrasts with the glassy state, where enough thermal motion is present to facilitate the completion of bonding in a greater number of cases. Thus two types of ESR centre must be present at the moment of preparation of the films.

The fact that only one ESR signal is produced in  $a\text{-SiO}$  thin films can be explained by noting first that these paramagnetic centres, unlike those in  $v\text{-SiO}_2$ , will most probably not be intimate pairs. Thus the  $\text{Si}_3^0$  defect will give rise to the  $\text{O}_3^+$  centre by reacting with the abundantly available neighbouring  $\text{O}_2^0$  sites as before. That this reaction is actually exothermic is seen by first evaluating the energy difference between the two sets of defects ( $\text{Si}_4^0, \text{O}_3^+$ ) and ( $\text{Si}_3^0, \text{O}_2^0$ ). Reference to Fig. 4 shows that this is equal to  $-E'_b - E_b$ , which is of the order of  $-10\text{ eV}$ . One must next take into account the fact that the production of the "free" electron requires some energy expenditure. This is because the charge creation process involves the bond-

ing of a silicon  $sp^3$  orbital with an oxygen p orbital already containing two electrons (the lone pair). This necessitates the elevation of one electron to a higher energy level, perhaps the antibonding level, for its complete removal from the site. In the solid state this may mean either a transfer of this electron to another site (which was a neighbouring  $\text{O}_2^0$  site in the case of  $v\text{-SiO}_2$ ) or elevation to the conduction band. Whatever this process is, it is plain that an upper bound for the energy expended is certainly provided by the band gap of  $\text{SiO}_2$ , which is no greater than  $9\text{ eV}$  [41]. Thus Step 2 above is exothermic and will proceed to completion.

Unlike the  $v\text{-SiO}_2$  case, the formation of  $\text{O}_1^-$  via step 3 is highly unlikely because the electron liberated in Step 2 will have a low probability of finding the  $\text{O}_1^0$  site. The net result is the survival of  $\text{O}_1^0$  (or OHC) as the only one of two possible paramagnetic centres mentioned above, as well as the creation of the non-paramagnetic  $\text{O}_3^+$  centre. The peroxy radical does not appear to exist in the films, as its ESR signal should appear as a broadening of the OHC peak [38], an effect not noted in the current results.

It must be emphasized that the above proposal is one of several possible explanations for the ESR response of  $a\text{-SiO}$  thin films, and additional evidence is required to substantiate it. Such evidence may be provided by the IR response of the  $\text{O}_3^+$  centre. Calculations carried out by Lucovsky [27] show that this centre possesses an IR band at  $620\text{ cm}^{-1}$ . The current investigations [1] do show a feature in the  $600$  to  $700\text{ cm}^{-1}$  region of the IR spectrum. However, more work needs to be done to establish its identity.

In summary, the IR band at  $876\text{ cm}^{-1}$  shows the presence of either  $\text{O}_1^0$  or  $\text{O}_1^-$ , while the feature in the  $600$  to  $700\text{ cm}^{-1}$  region probably indicates the presence of  $\text{O}_3^+$ . This, combined with the ESR result pointing to the presence of  $\text{O}_1^0$  and  $\text{O}_3^+$  centres, leads one to conclude that the defect centres in  $a\text{-SiO}$  thin films are predominantly these latter pairs.

### 3.4. Trends in $\text{SiO-CeO}_2$ films

As the concentration of  $\text{CeO}_2$  increases in the films, the  $876\text{ cm}^{-1}$  band weakens and disappears at the  $44\text{ mol } \%$  SiO composition [1], and a rapid reduction of the ESR signal also results [3]. However, the IR feature in the  $600$  to  $700\text{ cm}^{-1}$  region remains until the SiO concentration in the films falls below the  $30\text{ mol } \%$  SiO composition. Evidently the  $\text{Ce}^{4+}$  ions bond with the  $\text{O}_1^0$  centres, reducing the ESR and the  $876\text{ cm}^{-1}$  IR signals together. The  $\text{O}_3^+$  centres must remain in the samples till the concentration of SiO becomes too low for their formation. Annealing provides further support for the identification of the latter IR band with the  $\text{O}_3^+$  centre, for although the  $876\text{ cm}^{-1}$  band is weakened after annealing, the other band is hardly affected. This is to be expected if this band is indeed due to an  $\text{O}_3^+$  centre, which ought not to be affected by heat treatment.

### 3.5. Assignment of UV bands

The possible presence of defect-related minima among the weak absorption bands observed in the optical

transmission edges of Figs 2 and 3 may be used as additional confirmation of the chemical make-up of the series of films. According to calculations carried out by O'Reilly and Robertson [21] the possible defects in  $v\text{-SiO}_2$  would produce absorptions at 2 eV (620 nm) due to  $\text{O}_1^0$ , 5 to 6 eV (200 to 250 nm) due to the peroxy radical, 7.6 eV (160 nm) due to any of several possible charged centres, and 5.85 eV (210 nm) due probably to neutral oxygen vacancies. Since a-SiO has been shown to contain only  $\text{O}_1^0$  and  $\text{O}_3^+$  centres in significant amounts, one only expects absorption bands at 2 and 7.6 eV, both of which values lie outside the range of energies considered here. The bands actually present in the current series occur at 4.3 eV (290 nm), 5.4 eV (230 nm) and 6.2 eV (200 nm). Of these, the 290 nm minimum is possibly due to defects. Because it does not appear either in the a-SiO or the a-CeO<sub>2</sub> spectra, it may thus point to the formation of new chemical bonds and/or defect centres in the films.

#### 4. Conclusions

UV results support the view first derived from IR results that there is formation of new chemical bonding in the first group of films (ranging in composition between 78 and 51 mol% SiO). These latter results also provide independent evidence for the existence of either  $\text{O}_1^0$  or  $\text{O}_1^-$  defect centres, and possibly also of  $\text{O}_3^+$  centres, in a-SiO thin films. ESR results show that the centres in a-SiO must be predominantly  $\text{O}_1^0$  and  $\text{O}_3^+$ .

The  $\text{Ce}^{4+}$  ions present in the mixed films bond themselves with the  $\text{O}_1^0$  centres of the a-SiO, thus reducing the ESR signal concurrently with the IR band at  $876\text{ cm}^{-1}$ .

The identity of the optical absorption bands in the spectra may be used to provide additional indication of Ce-Si-type bonds in the films.

#### References

1. A. SINGH and C. A. HOGARTH, *J. Mater. Sci.* **23** (1987) 1090.
2. Z. T. AL-DHHAN and C. A. HOGARTH, *Int. J. Electron.* **63** (1987) 707.
3. A. RAZZAQ, C. A. HOGARTH and K. A. LOTT, *Phys. Status Solidi (b)* **141** (1987) K67.
4. C. A. HOGARTH and Z. T. AL-DHHAN, *Phys. Status Solidi (b)* **137** (1986) K157.
5. S. K. J. AL-ANI and J. BEYNON, *Phys. Educ.* **20** (1985) 274.
6. J. I. PANKOVE, "Optical Processes in Semiconductors" (Prentice-Hall, Englewood Cliffs, New Jersey, 1971).

7. G. A. N. CONNELL, in "Amorphous Semiconductors" (Topics in Applied Physics, Vol. 36), edited by M. H. Brodsky (Springer, Berlin, New York, 1979) Ch. 4.
8. M. KASTNER, *Phys. Rev. Lett.* **28** (1972) 355.
9. E. MOOSER and W. B. PEARSON, "Progress in Semiconductors," Vol. 5 (Heywood, London, 1960) p. 104.
10. M. H. COHEN and V. HEINE, *Phil. Mag.* **7** (1958) 395.
11. W. MEYER, *Z. Elektrochem.* **50** (1944) 274.
12. E. FRIEDERICH, *Z. Phys.* **31** (1925) 813.
13. *Idem, ibid.* **34** (1925) 637.
14. A. F. JOFFÉ and A. R. REGEL, *Prog. Semicond.* **4** (1960) 237.
15. H. R. PHILIPP, *J. Phys. Chem. Solids* **32** (1971) 1935.
16. Z. T. AL-DHHAN, private communications (1987).
17. J. TAUC, R. GRIGOROVICI and A. VANCU, *Phys. Status Solidi* **15** (1966) 627.
18. E. A. DAVIS and N. F. MOTT, *Phil. Mag.* **22** (1970) 903.
19. D. WEAIRE and M. F. THORPE, *Phys. Rev. B* **4** (1971) 2508.
20. *Idem, ibid.* **4** (1971) 3518.
21. E. P. O'REILLY and J. ROBERTSON, *ibid.* **27** (1980) 3780.
22. D. L. GRISCOM, *J. Non-Cryst. Solids* **40** (1980) 211.
23. N. F. MOTT, *Adv. Phys.* **26** (1977) 363.
24. *Idem, J. Non-Cryst. Solids* **40** (1980) 1.
25. G. N. GREAVES, *Phil. Mag. B* **37** (1978) 447.
26. *Idem, J. Non-Cryst. Solids* **32** (1979) 295.
27. G. LUCOVSKY, *Phil. Mag. B* **39** (1979) 513.
28. *Idem, ibid. B* **41** (1980) 457.
29. *Idem, Phil. Mag. B* **39** (1979) 531.
30. *Idem, J. Non-Cryst. Solids* **35/36** (1980) 825.
31. P. W. ANDERSON, *Phys. Rev. Lett.* **34** (1975) 953.
32. R. A. STREET and N. F. MOTT, *ibid.* **35** (1975) 1293.
33. M. KASTNER, D. ADLER and H. FRITZSCHE, *ibid.* **37** (1976) 1504.
34. M. KASTNER and H. FRITZSCHE, *Phil. Mag. B* **37** (1978) 199.
35. D. L. GRISCOM, in "The Physics of SiO<sub>2</sub> and Its Interfaces", edited by S. T. Pantelides (Pergamon, New York, 1978) p. 232.
36. G. N. GREAVES, *Phil. Mag. B* **37** (1978) 447.
37. *Idem*, in "The Physics of SiO<sub>2</sub> and Its Interfaces", edited by S. T. Pantelides (Pergamon, New York, 1978) p. 268.
38. E. J. FRIEBELE, D. L. GRISCOM and M. STAPEL-BROEK, *Phys. Rev. Lett.* **42** (1979) 1346.
39. D. L. GRISCOM and E. J. FRIEBELE, *Phys. Rev. B* **24** (1981) 4896.
40. K. L. CHOPRA, "Thin Film Phenomena" (McGraw-Hill, New York, 1969).
41. N. F. MOTT, in "The Physics of SiO<sub>2</sub> and Its Interfaces" edited by S. T. Pantelides (Pergamon, New York, 1978) p. 1.

Received 7 July

and accepted 27 July 1987